International Journal of Nanomedicine

Dovepress
Taylor & Francis Group

Open Access Full Text Article

ORIGINAL RESEARCH

Nanomicellar Prodrug Delivery of Glucose-Paclitaxel: A Strategy to Mitigate Paclitaxel Toxicity

Didi Yan[1], Xinyue Ma[1], Yixin Hu[1], Guogang Zhang[1], Beibei Hu[1], Bo Xiang[2], Xiaokun Cheng[1,3], Yongshuai Jing[1], Xi Chen[1,4]

[1]College of Chemical and Pharmaceutical Engineering, Hebei University of Science and Technology, Shijiazhuang, 050018, People's Republic of China; [2]Department of Psychiatry, Fundamental and Clinical Research on Mental Disorders Key Laboratory of Luzhou, Affiliated Hospital of Southwest Medical University, Luzhou, 646000, People's Republic of China; [3]New Drug Research & Development Co., Ltd., North China Pharmaceutical Group Corporation, Shijiazhuang, 050015, People's Republic of China; [4]Hebei Research Center of Pharmaceutical and Chemical Engineering, Shijiazhuang, 050018, People's Republic of China

Correspondence: Xi Chen, College of Chemical and Pharmaceutical Engineering, Hebei University of Science and Technology, 26 Yuxiang Road, Shijiazhuang, 050018, People's Republic of China, Tel +86-15203319951, Email chenxi0310@163.com

Background: Paclitaxel-induced blood system disorders and peripheral neuropathy impede the progress of new formulations in clinical trials.

Purpose of Study: To mitigate these adverse effects by developing and validating a prodrug strategy that encapsulates a glucose-paclitaxel conjugate within nanomicelles.

Material and Methods: Succinic anhydride was used as a bridge to couple C2'-paclitaxel with methyl 2'-glucopyranose and prepare a glucose-paclitaxel conjugate. Nanomicelles were prepared via solid-phase dispersion, and dynamic light scattering was used to determine their average diameter and the polydispersity index. High-performance liquid chromatography (HPLC) was employed to evaluate drug-loading capacity and encapsulation efficiency. Pharmacokinetic studies and in vivo toxicity assays were performed in Sprague-Dawley (SD) rats.

Results: The nanomicellar product exhibited a spherical shape with a particle size distribution between 20–60 nm, a PDI of 0.26 ± 0.01, and an encapsulation efficiency of 95.59 ± 1.73%. The pharmacokinetic profile of glucose-paclitaxel nanomicelles in SD rats was markedly different from that of the paclitaxel solution group. Notably, the plasma drug concentration of glucose-paclitaxel nanomicelles was significantly higher than the paclitaxel solution 15 minutes post-administration, with a V_z at only 40% of that of the paclitaxel solution, while the $AUC_{0-\infty}$ was five times greater than that of the paclitaxel solution. Ultimately, glucose-paclitaxel nanomicelles effectively alleviated blood system disorders and peripheral neuropathy in SD rats.

Conclusion: The encapsulation of glucose-paclitaxel conjugates within nanomicelles presents a viable solution to the dose-limiting toxicities associated with paclitaxel, offering new perspectives on safety for the development of paclitaxel-based therapeutics.

Keywords: glucose-paclitaxel conjugate, nanomicelles, pharmacokinetics, toxicity of paclitaxel

Introduction

Since the approval of Taxol® (the first generation paclitaxel formulation) by the FDA in 1992 for treating advanced ovarian cancer, the clinical limitations of this drug have become progressively evident.[1] Aiming to solve paclitaxel's low solubility in water, Taxol® incorporates drugs in a solution containing polyethoxylated castor oil (CrEL) and ethanol at 1:1 (v/v), which is associated with hypersensitivity reactions, as well as various inconveniences during clinical administration.[2] The administration time must be extended to dilute the solvent, and premedication with antihistamines and glucocorticoids is required to mitigate hypersensitivity reactions. However, corticosteroids can interfere with the immune response by blocking the programmed cell death ligand (PD-(L)) 1 during cancer treatment, which is unfavorable for combination therapy with paclitaxel.[3] Moreover, Taxol® must be prepared in a non-polyvinyl chloride administration set and infused with in-line filtration to prevent the precipitation of leaching plasticizers,[4] which undoubtedly increases both the risk and cost associated with therapy. In addition to the need for premedication and special administration devices, CrEL can alter paclitaxel

Received: 13 November 2024
Accepted: 30 January 2025
Published: 17 February 2025

pharmacokinetics by trapping the compound in the CrEL micelles.[5] It leads to a reduced fraction of free paclitaxel available for clearance and distribution, consequently resulting in nonlinear pharmacokinetic behavior,[6] thereby making it difficult to accurately adjust the dosage of drugs.

To circumvent these unfavorable effects, new formulations of paclitaxel have been established as substitutes for CrEL applications. Several new drug delivery systems using nanoparticles,[7,8] microspheres,[9] micelles,[10–14] liposomes,[15–17] emulsion,[18] and prodrugs[19–22] have been investigated in clinical studies, with some already approved for their superior clinical benefits compared with Taxol®. For example, Abraxane, also referred to as nab-paclitaxel, a nanoparticle albumin-bound paclitaxel formulation, can eliminate the need for any solvent, thus demonstrating a shorter administration time (30 min) and lower infusion volume, alleviating the danger of leaching plasticizers from the infusion set, and does not require steroid premedication.[23–25] This formulation allows for the administration of a higher dose of paclitaxel, leading to improved response against tumor and prolonged time to tumor progression compared to Taxol®.[26] Genexol-PM, the CrEL-free polymeric micelle, can be safely given as a 1-hour infusion without the need for premedication. It offers comparable effectiveness to other treatments, while maintaining a manageable safety profile.[18] GRN1005, a conjugate of paclitaxel and Angiopep-2 designed to increase drug delivery to the brain,[27] displays well-tolerated and linear pharmacokinetic behavior, showing activity in a Phase I study on recurrent glioma.[20]

Although new paclitaxel formulations have gained benefits in terms of absence of hypersensitivity reactions and convenient administration, adverse effects induced by paclitaxel itself mainly refer to blood system disorders and peripheral neuropathy, often interfered with dose scheduling or even discontinued subsequent treatment. Previous studies have demonstrated that paclitaxel at physiological concentrations interrupts the division of precursor cells within the bone marrow with time-dependent effects on the duration of paclitaxel exposure.[28–30] Clinical pharmacokinetic studies of paclitaxel have suggested that patients with a higher overall systemic drug exposure are more likely to experience peripheral neuropathy.[31,32] Therefore, it is important to explore innovative delivery strategies that can constrict the extensive systemic distribution of paclitaxel, thereby preventing excessive exposure to high concentrations of free drug in the blood circulation, which directly affects the bone marrow. Small sugar molecule drug conjugates have been designed as prodrugs to improve water solubility and target the delivery of anticancer compounds via the overexpression of glucose transporters in cancer cells.[33,34] Several types of glycoconjugates of paclitaxel have been synthesized and proven to be superior due to their better water solubility and increased antitumor activity compared to paclitaxel, as evidenced by in vitro cytotoxicity studies.[35,36] However, these prodrugs manifest a rapid release of paclitaxel in the serum, thereby resulting in excessive paclitaxel exposure in the blood circulation, which complicates the management of blood system disorders and peripheral neuropathy induced by paclitaxel.

One way to counteract this premature cleavage of the covalent bond between the sugar ligand and paclitaxel is to fabricate prodrugs into nanomicelles. Nanomicelles exhibit a core-shell structure that encapsulates insoluble drugs into the core area to increase solubility. In addition, nanomicelles protect the covalent bonds of prodrugs from degradation by enzymes in the circulation, thus decreasing free paclitaxel exposure within the bloodstream. This may be beneficial in managing blood system disorders and peripheral neuropathy.

To verify this hypothesis, we synthesized a glucose-paclitaxel conjugate and encapsulated it within nanomicelles, comparing its pharmacokinetic profile, effects on blood system disorders, and peripheral neuropathy in SD rats with those of paclitaxel dissolved in CrEL and ethanol.

Materials and Methods

Materials

N,N'-Dicyclohexylcarbodiimide (DCC), 4-Dimethylaminopyridine (DMAP) were sourced from Shanghai Yuanye Biotechnology Co., Ltd.; Paclitaxel (purity, 99.5%) was sourced from Xi 'an Haoxuan Biotechnology Co., Ltd.; Methyl-4,6-O-benzylidene-α-D-glucopyranoside (MBG) (purity, 99.6%) was sourced from Shanghai Ling Kai Pharmaceutical Technology Co., Ltd.; tetrabutylammonium bromide (TBAB), dipivaloylmethane and benzyl bromide (purity, 99.0%) were sourced from Shanghai McLean Biochemical Technology Co., Ltd.; Succinic anhydride (purity, 99.0%) and silver oxide were purchased from West Asia Chemical Technology (Shandong) Co., Ltd. (Shandong, China); Pd/C mixture was sourced from Shanghai Bide Pharmaceutical Technology Co., Ltd. Methoxy poly (ethylene glycol)$_{2k}$-poly (D, L-lactide)$_{3k}$ (mPEG2000-PDLLA3000) was

obtained from Guangzhou Weihua Biotechnology Co. Ltd. Norethisterone was purchased from the China Food and Drug Control Institute. Heparin sodium was obtained from Beijing Solaibao Technology Co. Ltd. Petroleum ether (boiling temperature of 60–90 °C), ethyl acetate, and n-hexane (Hex) were purchased from Shanghai Titan Technology Co., Ltd. All other reagents used were of analytical or chromatographic grade.

SD rats weighing 180–200 g were purchased from Beijing Huafukang Biotechnology Co. Ltd. The protocols for the animal experiments were approved by the Institutional Animal Care and Use Committee of the Experimental Animal Ethics Committee of Southwest Medical University (20230216–003).

Synthesis of Glucose-Paclitaxel Prodrug

$FeCl_3$ (25 mg, 0.15 mmol) was dissolved in anhydrous acetonitrile (MeCN) (10 mL) in a three-necked flask, then dipivaloylmethane (63 μL, 0.3 mmol), Ag_2O (248 mg, 1.0 mmol), tetrabutylammonium bromide (50 mg, 0.15 mmol) were supplemented. After stirring (49 °C, 0.5 h), MBG (282 mg, 1.0 mmol) and benzyl bromide (180 μL, 1.5 mmol) were added to the solution. The products were stirred (49 °C for 4.36 h). The solvent was subsequently evaporated under reduced pressure, and the residue was purified by silica gel column chromatography and eluted with ethyl acetate/petroleum ether (1:12, v/v) to obtain the white solid 1 (166 mg, 45%). ^{1}H NMR (500 MHz, $CDCl_3$) δ 7.52–7.47 (m, 2H), 7.41–7.31 (m, 8H), 5.52 (s, 1H), 4.79 (d, J = 12.2 Hz, 1H), 4.71 (d, J = 12.2 Hz, 1H), 4.62 (d, J = 3.6 Hz, 1H), 4.26 (dd, J = 10.2, 4.8 Hz, 1H), 4.16 (t, J = 9.3 Hz, 1H), 3.82 (td, J = 9.9, 4.8 Hz, 1H), 3.70 (t, J = 10.3 Hz, 1H), 3.52–3.45 (m, 2H), 3.38 (s, 3H). (see Supporting Information for the NMR spectrum, Figure S1; the Mass spectrum, Figure S2).

Succinic anhydride (202.2 mg, 2.0 mmol) was supplemented into mixture consisting of DMAP (25 mg, 0.20 mmol) and compound 1 (149.6 mg, 0.4 mmol) within 6 mL CH_2Cl_2, while being constantly stirred (room temperature, 24 hours). The reaction mixture was extracted with HCl 0.1 mol/L and evaporated under pressure. The residue was purified using silica gel column chromatography, eluted with ethyl acetate/petroleum ether (1:12, v/v), and dried under vacuum to yield white solid powder 2 (179.8 mg, 95%). ^{1}H NMR (500 MHz, $CDCl_3$) δ 7.44–7.39 (m, 2H), 7.32 (dtd, J = 10.8, 7.0, 3.6 Hz, 8H), 5.57 (t, J = 9.7 Hz, 1H), 5.44 (s, 1H), 4.68–4.59 (m, 3H), 4.26 (dd, J = 10.2, 4.9 Hz, 1H), 3.91–3.84 (m, 1H), 3.70 (t, J = 10.3 Hz, 1H), 3.60–3.51 (m, 2H), 3.39 (s, 3H), 2.67–2.55 (m, 4H). (see Supporting Information for the NMR spectrum, Figure S3).

A solution of paclitaxel (51.5 mg, 0.06 mmol), DMAP (7.4 mg, 0.06 mmol), DCC (75 mg, 0.36 mmol) in tetrahydrofuran (THF) (4 mL) was supplemented to the mixture consisting of compound 2 (85 mg, 0.18 mmol) in THF (4 mL), then sent for constant stirring (room temperature, 24 h). The residue was purified by silica gel column chromatography eluted with ethyl acetate/Hex (1:10, v/v) and dried under vacuum to yield white solid powder 3 (39.7 mg, 50%). ^{1}H NMR (500 MHz, $CDCl_3$) δ 8.13 (t, J = 5.9 Hz, 2H), 7.75 (d, J = 7.1 Hz, 2H), 7.61 (t, J = 5.7 Hz, 1H), 7.57–7.45 (m, 4H), 7.45–7.17 (m, 16H), 6.97 (dd, J = 9.0, 3.9 Hz, 1H), 6.20 (q, J = 9.2, 6.7 Hz, 2H), 5.91 (dt, J = 8.7, 3.7 Hz, 1H), 5.66 (t, J = 5.7 Hz, 1H), 5.61–5.50 (m, 1H), 5.43 (d, J = 4.1 Hz, 2H), 4.93 (d, J = 9.4 Hz, 1H), 4.71 (dd, J = 12.5, 3.9 Hz, 1H), 4.67–4.54 (m, 2H), 4.29 (dtd, J = 22.2, 10.7, 9.9, 5.6 Hz, 3H), 4.18 (dd, J = 8.5, 3.7 Hz, 1H), 4.12 (dd, J = 9.3, 5.1 Hz, 1H), 3.92–3.80 (m, 1H), 3.80–3.64 (m, 2H), 3.53 (dt, J = 14.4, 7.3 Hz, 2H), 3.40 (d, J = 3.9 Hz, 3H), 2.83–2.42 (m, 4H), 2.40 (d, J = 3.9 Hz, 2H), 2.36–2.26 (m, 1H), 2.21 (d, J = 3.9 Hz, 3H), 2.04 (d, J = 4.2 Hz, 1H), 1.84 (s, 3H), 1.66 (d, J = 4.0 Hz, 3H), 1.41–1.30 (m, 2H), 1.31–1.17 (m, 6H), 1.12 (d, J = 4.1 Hz, 3H). (see Supporting Information for the NMR spectrum, Figure S4).

The mixture of compound 3 (46 mg, 0.035 mmol), Pd/C (25 mg, 0.23 mmol) in methanol (MeOH) (4 mL) was sent for stirring (room temperature, hydrogen atmosphere, 12 h). The reaction mixture was filtered using diatomite, and the residue was purified by silica gel column chromatography, eluted with ethyl acetate/hexane (20:1, v/v), and dried under vacuum to obtain white solid powder 4 (31 mg, 79%). ^{1}H NMR (500 MHz, $CDCl_3$) δ 8.20–8.09 (m, 2H), 7.80 (d, J = 7.6 Hz, 2H), 7.60 (t, J = 7.4 Hz, 1H), 7.50 (q, J = 7.3 Hz, 3H), 7.44–7.37 (m, 6H), 7.37–7.31 (m, 1H), 7.13 (d, J = 9.2 Hz, 1H), 6.29 (s, 1H), 6.20 (t, J = 9.0 Hz, 1H), 5.97 (dd, J = 9.4, 3.2 Hz, 1H), 5.68 (d, J = 7.0 Hz, 1H), 5.48 (d, J = 3.4 Hz, 1H), 5.07–4.93 (m, 2H), 4.71 (d, J = 3.8 Hz, 1H), 4.43 (dd, J = 10.9, 6.5 Hz, 1H), 4.31 (d, J = 8.5 Hz, 1H), 4.20 (d, J = 8.5 Hz, 1H), 4.12 (q, J = 7.1 Hz, 2H), 3.80 (d, J = 7.0 Hz, 1H), 3.72 (dd, J = 6.7, 3.7 Hz, 2H), 3.57 (t, J = 9.5 Hz, 1H), 3.51–3.37 (m, 5H), 2.89–2.62 (m, 4H), 2.55 (dd, J = 10.6, 5.0 Hz, 1H), 2.48 (s, 3H), 2.35 (dd, J = 15.4, 9.5 Hz, 1H), 2.23

(s, 3H), 2.16 (dd, J = 15.6, 8.9 Hz, 1H), 2.04 (s, 3H), 1.91–1.86 (m, 4H), 1.68 (s, 3H), 1.22 (s, 3H), 1.14 (s, 3H). (see Supporting Information for the NMR spectrum, Figure S5; the Mass spectrum, Figure S6).

Physical Properties of Glucose-Paclitaxel

Determination Solubility of Glucose-Paclitaxel

The solubility of paclitaxel and glucose-paclitaxel were measured after shaking the flask, and suspensions of each compound in excess were prepared in 10 mL of pure water, 5% glucose solution, or physiological saline and stirred (25 °C for 72 h). The product was centrifuged (10000 rpm, 10 min) to remove the insoluble fraction and then filtered through a 0.22 μm filter. The compound concentration in the saturated solutions was quantified using HPLC (Agilent Technologies Singapore Inc., Yishun, Singapore) and calculated through interpolation based on the calibration curve. Solubility values represent the average of three independent tests.

Plasma Stability of Glucose-Paclitaxel in vitro

The plasma stability was estimated by preparing a 10 μL methanol solution containing glucose-paclitaxel (0.5 $mg{\cdot}mL^{-1}$) and subsequently added to 1000 μL rat blank plasma in triplicate. The system was swirled for 30s and incubated at 37 °C. Then, 100 μL of the sample extracted from the system was collected at time points of 0, 5, 15, 20, 30, 60, 90, 120, and 240 min, and 500 μL methanol with 10 μL of internal standard norethindrone solution (100 $\mu g{\cdot}mL^{-1}$) was added. The samples were vortexed (5 minutes) and centrifuged (10000 rpm for 15 minutes). The supernatant was collected and evaporated to dryness by using a nitrogen evaporator at 45 °C. Thereafter, the samples were reconstituted in 50% acetonitrile:50% water (100 μL) and transferred to HPLC vials for analysis.

The stability of the glucose-paclitaxel nanomicelles in plasma was determined in the same way as described above.

Preparation of Nanomicelles

The nanomicelles were prepared via solid-phase dispersion.[37–39] In brief, glucose-paclitaxel and mPEG2000-PDLLA3000 (in a 1:8 mass ratio) were dissolved in acetonitrile and evaporated using a 250 mL eggplant-shaped rotary evaporator (Tianjin Chengsheng Glass Instrument Co., Tianjin, China) while stirring (37 rpm and 50 °C). The resulting dried film was then redispersed in 5 mL normal saline at 50 °C to allow the self-assembly of nanomicelles. Finally, the nanomicelles were filtered utilizing syringe filter sized 0.22 μm (Jinteng Experimental Equipment Co., Tianjin, China) to form the resulting product.

Characterization of Nanomicelles

Morphology and Size

The polydispersity index (PDI), particle size, Zeta potential and morphology are the fundamental properties of nanomicelles. The average diameter and PDI were determined by dynamic light scattering (DLS) using a Zetasizer Nano ZS90 analyzer (Malvern, Worcestershire, UK) assisted by a red diode laser (4 mW, λ = 632.8 nm at scattering angle of 90). Samples for zeta potential measurements were placed in specialized cuvettes capable of conducting current during analysis. The morphology of the glucose-paclitaxel nanomicelles was observed by transmission electron microscopy (TEM) (JEM-2100, JEOL Co., Tokyo, Japan). The nanomicelles were then diluted and positioned on a nitrocellulose-covered copper grid. Negatively stained phosphotungstic acid samples were dried at room temperature.

Efficiencies of Drug Loading (DL) and Encapsulation (EE)

The ability of the mPEG-PDLLA nanomicelles to encapsulate glucose-paclitaxel was assessed using the DL efficiency and EE. Three batches of nanomicelles were prepared according to the method described in section *Preparation of nanomicelles*. The 0.22 μm syringe filter was rinsed with methanol to collect the non-encapsulated glucose-paclitaxel. DL efficiency and EE of glucose-paclitaxel nanomicelles were determined using the following equations, with results presented as mean ± standard deviation.

$$EE(\%) = \frac{\text{Total mass of drug} - \text{Mass of free drug}}{\text{Total mass of drug}} \times 100\% \quad (1)$$

$$\mathrm{DL}(\%) = \frac{\text{Total mass of drug} - \text{Mass of free drug}}{\text{Total mass of nanomicelles}} \times 100\% \quad (2)$$

The Placement Stability of Nanomicelles

The placement stability of glucose-paclitaxel nanomicelles were evaluated after diluting within PBS (pH7.4). The nanomicelles were stored at 25°C and 4°C for 28 days. Particle size measurements were conducted at days 1, 2, 4, 8, 16, and 28. Zeta potential were measured at days 1 and 28.

Biocompatibility Evaluation

To evaluate biocompatibility, blood was collected from SD rats, and was diluted with saline. The blood sample was then centrifuged at a low speed of 4000 rpm for 6 min to separate the supernatant. This process was repeated 3 times until the supernatant became clear, leaving a purified red blood cells (RBCs). The obtained RBCs were used to prepare a 2% RBC saline suspension. The 2% RBC saline suspension was mixed with saline (negative control sample 1), distilled water (positive control sample 7), or glucose-paclitaxel nanomicelles at concentrations of 20, 40, 60, 80, 100μg·mL^{-1} (samples2-6). After incubation at 37°C for 5 hours, the OD value was quantified using a UV spectrophotometer to evaluate hemolytic effects and biocompatibility.

$$\text{Hemolysis rate}(\%) = \frac{\mathrm{OD}_{sample} - \mathrm{OD}_{negative}}{\mathrm{OD}_{positive} - \mathrm{OD}_{negative}} \times 100\% \quad (3)$$

In vivo Pharmacokinetics Analyses

Six SD rats were randomly divided into groups A and B, each group comprised 3 rats. Paclitaxel solution (CrEL: dehydrated ethanol = 1:1) and glucose-paclitaxel nanomicelles were injected via the tail vein at a paclitaxel-equivalent (paclitaxel-equ) dose of 5 mg·kg^{-1} in groups A and B, respectively. Blood samples (200 μL) were obtained from the tail vein at specific time intervals (5 min, 15 min, 30 min, 1 h, 2 h, 4 h, 6 h, 8 h, 10 h, 12 h and 24 h). The samples were subsequently centrifuging (4000 rpm for 10 minutes) for extract the plasma. The drug content in the plasma was determined as described in Section Stability of glucose-paclitaxel in vitro.

The experimental data are expressed as the mean ± SD. Pharmacokinetic behavior was analyzed by operating a non-compartmental model using DAS2.0. Pharmacokinetic indicators were calculated as follows: AUC of the curve indicating plasma concentration-time from zero (time) to infinity ($AUC_{0-\infty}$) or the time point of the latest measurement (AUC_{0-t}), total body clearance (CL_z), volume of distribution (V_z), elimination half-life ($t_{1/2z}$), and mean residence time ($MRT_{0-\infty}$).[40]

In vivo Toxicity Assay

Paclitaxel-induced toxicity in blood system disorders and peripheral neuropathy was evaluated in SD rats. The rats were acclimatized for 7 days under laboratory conditions prior to the experimental study. After adapting to the environment, SD rats were randomly divided into paclitaxel solution or glucose-paclitaxel nanomicelle groups and then given 5 mg·kg^{-1} of paclitaxel or paclitaxel-equ via the tail vein. Blood samples (0.25 mL) were placed in EDTA K2 anticoagulant tubes before administration (6/12/24 h) and analyzed using an automatic animal blood cell analyzer (Mindray, Shenzhen, China).

Peripheral neuropathy was evaluated using a heat stimulus-induced tail-flick pain test. The SD rats were randomly divided into paclitaxel solution group or glucose-paclitaxel nanomicelles group and then administered 5 mg·kg^{-1} paclitaxel or paclitaxel-equ via the tail vein. After calming to a quiet state, the rats were immersed in tail tips of approximately 5 cm in water at 50 °C. Tail-flick time was defined as the tail-flick latency. Tail-flick latency was measured before administration and 30/60/120/240 min post-injection.

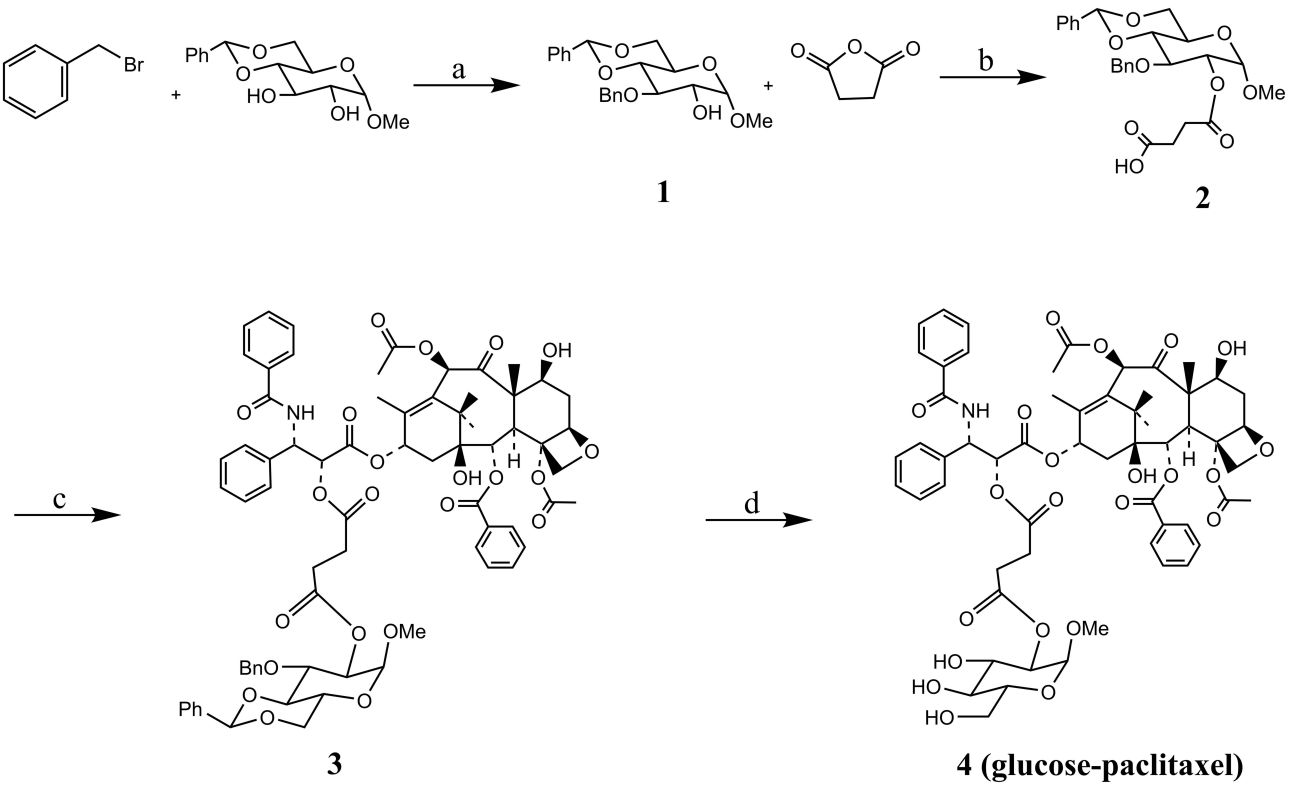

Figure 1 Synthetic route of glucose-paclitaxel. Reagents and conditions: (a) $FeCl_3$, Ag_2O, Dipivaloylmethane, TBAB, MeCN; (b) DMAP, CH_2Cl_2; (c) paclitaxel, DCC, DMAP, THF; (d) Pd/C, H_2, MeOH.

Statistical Analysis

Experimental data are expressed as the mean ±SD. Pharmacokinetic indicators were computed by operating a non-compartment model using DAS 2.0. Comparison analysis between cohorts relied on one-way analysis of variance (ANOVA) using SPSS statistical software, with significant differences noted as $*p < 0.05$, $**p < 0.01$.

Results

Design and Synthesis of Glucose-Paclitaxel Prodrug

The design and synthesis route of the glucose-paclitaxel conjugates are shown in Figure 1. The glucose-paclitaxel conjugate was synthesized via a simple esterification reaction using MBG, succinic anhydride, and paclitaxel as initiators. The structures of glucose-paclitaxel and its intermediates were validated by ^{1}H NMR and MS.

Physical Properties

The solubility of paclitaxel and glucose-paclitaxel conjugates are listed in Table 1. The aqueous solubility of the drug in the three media was 6–19 times that of the parent drug, indicating that paclitaxel prodrug solubility could be improved by glycosylated moieties. The maximum solubility of glucose-paclitaxel was 6.86 ± 0.98 μg·mL^{-1} in physiological saline, although this concentration still could not match the clinical concentration of paclitaxel.

Table 1 Solubility of Glucose-Paclitaxel and Paclitaxel (n = 3)

Compound	Pure Water (μg·mL^{-1})	Saline (μg·mL^{-1})	5% Glucose (μg·mL^{-1})
Paclitaxel	0.61 ± 0.02	0.66 ± 0.14	0.16 ± 0.06
Glucose-paclitaxel	3.93 ± 0.34	6.86 ± 0.98	3.05 ± 0.41

The plasma stability of the glucose-paclitaxel conjugates was then evaluated in vitro, and the concentration of the prodrug decreased over time, approaching zero at 60 min (Figure 2). The half-life time of glucose-paclitaxel in plasma was only 8.59 minutes, suggesting that the prodrug rapidly converted to paclitaxel in the blood, likely due to the influence by metabolic enzymes. In contrast, the half-life of glucose-paclitaxel in nanomicelles was 39.83 minutes, which is approximately five times longer than that of glucose-paclitaxel solution, indicating that nanomicelles could improve the prodrug circulation time in the bloodstream.

Characterization of Nanomicelles

Glucose-paclitaxel nanomicelles were prepared using a solid-phase dispersion method, and the properties of the resulting products were characterized sequentially after preparation. The nanomicelles appeared as a transparent solution with a light-blue hue under natural light (Figure 3).

The morphology of the nanomicelles was investigated using TEM, confirming the formation of spherical structures with a uniform size (Figure 4A). The particle size distribution ranged from 20–60 nm with a PDI of 0.26 ± 0.01 (Figure 4B). Using formulas (1) and (2), the EE of glucose-paclitaxel nanomicelles was calculated to be 95.59 ± 1.73%, while DL was 11.46 ± 0.68%. Both EE and DL of the nanomicelles were relatively stable, and no aggregation was observed in the TEM micrographs (at room temperature for 72 h or 4 °C for 7 days).

Figure 5 illustrates the particle size of glucose-paclitaxel nanomicelles stored at 25°C and at 4°C for a 28-day period. The Zeta potential were measured −3.35±0.26 mV at day 1 and −3.19±0.37 mV at day 28. These data reveal no significant alterations throughout the storage duration, demonstrating the nanomicelles excellent stability under both temperature conditions.

In the biocompatibility evaluation process of 37°C incubation, the negative control sample 1 treated with saline showed no hemolysis. Conversely, the positive control sample 7 showed complete hemolysis. In addition, no visible hemolysis was observed in samples 2–6, and the hemolysis rates of samples 2–6 remained below 5%, indicating the good biocompatibility of glucose-paclitaxel nanomicelles (Figure 6).

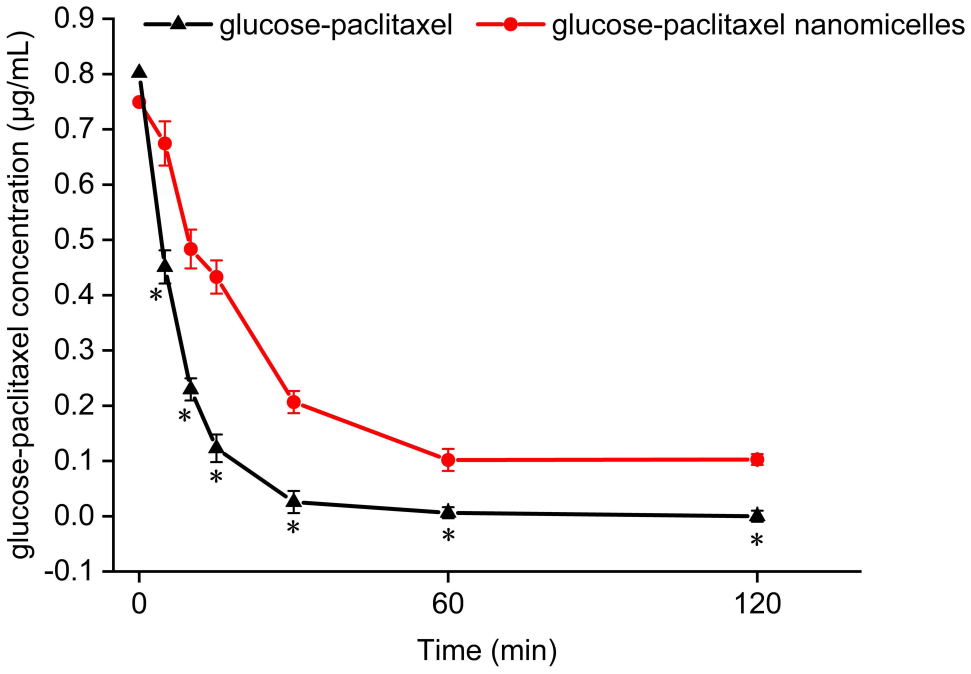

Figure 2 The concentration of glucose-paclitaxel in plasma as a function of incubation time (*$p < 0.05$).

https://doi.org/10.2147/IJN.S500999

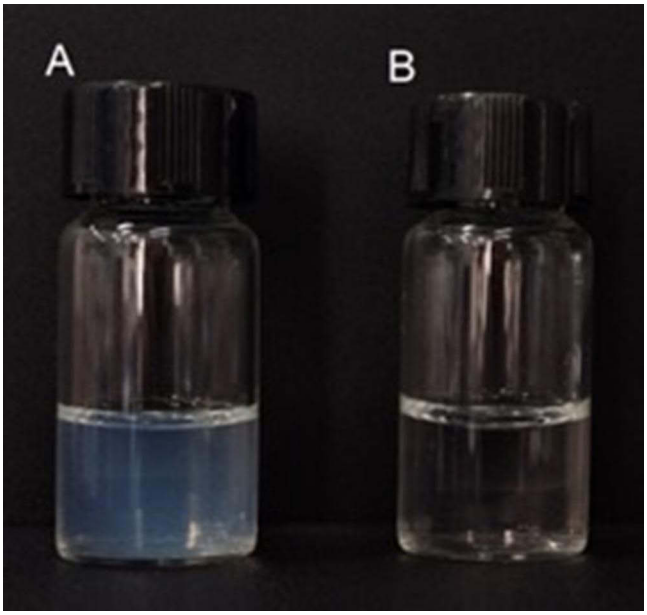

Figure 3 Appearance of glucose-paclitaxel nanomicelles solution (**A**) and H_2O (**B**).

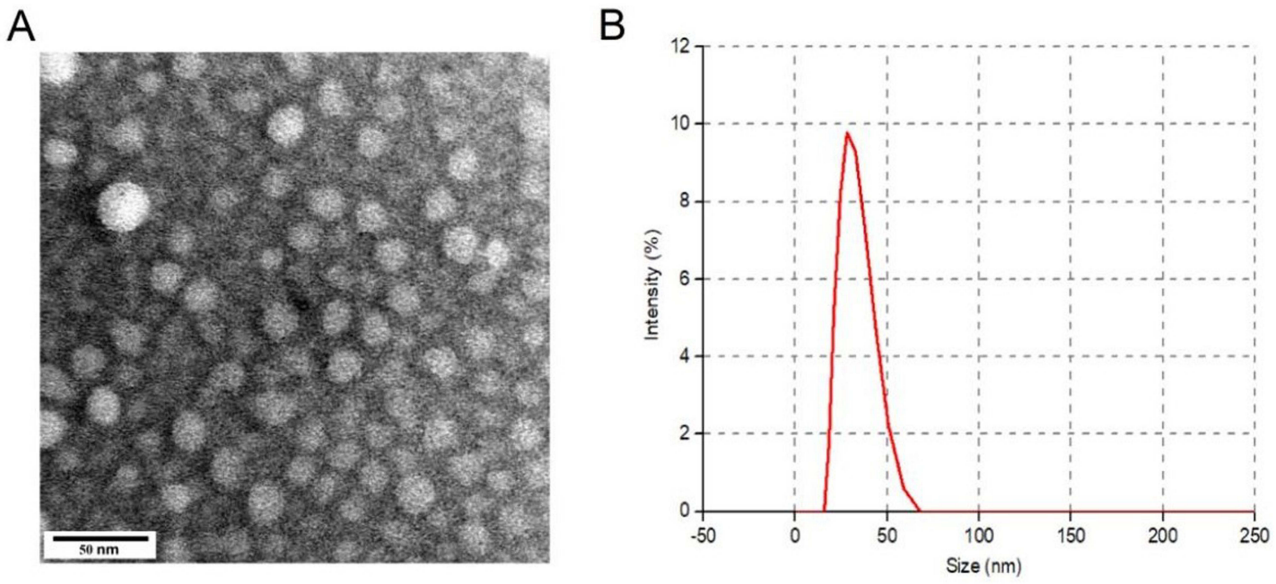

Figure 4 The morphology and size of glucose-paclitaxel nanomicelles. (**A**) TEM images of glucose-paclitaxel nanomicelles (scale bar: 50 nm). (**B**) Size distributions of glucose-paclitaxel nanomicelles, average particle size: 33.47 ± 1.74 nm (n = 3).

In Vivo Pharmacokinetics Analysis

The plasma concentration-time profiles of the glucose-paclitaxel nanomicelles and paclitaxel solution are shown in Figure 7, and the relevant pharmacokinetic indicators are shown in Table 2. As shown in Figure 7A, the concentration of glucose-paclitaxel declined drastically within the initial 30 min, approaching zero after 8 h. In Figure 7B, the concentration of paclitaxel increased to C_{max} at 15 min, after which the plasma paclitaxel concentration remained higher than that of the prodrug, as plotted in Figure 7C. As shown in Figure 7D, the observed drug pharmacokinetic behavior indicated that the drug concentration level of glucose-paclitaxel nanomicelles was higher than that of the paclitaxel solution after administration, in other words, the prodrug in the nanomicelles limited the distribution of paclitaxel into tissues.

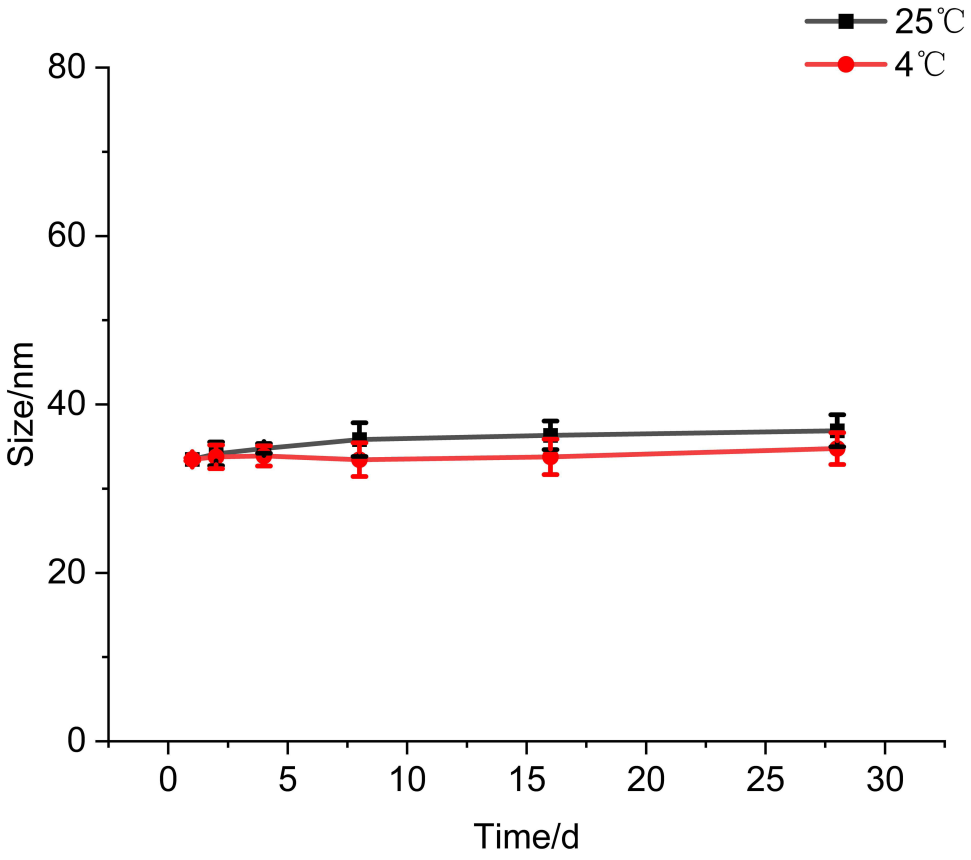

Figure 5 The placement stability of glucose-paclitaxel nanomicelles (n= 3).

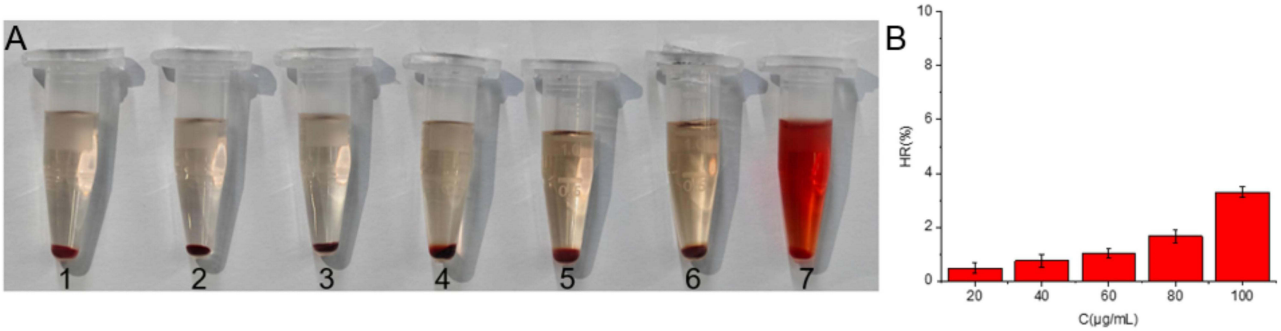

Figure 6 Biocompatibility Evaluation of glucose paclitaxel nanomicelles. (**A**) Qualitative and (**B**) quantitative analysis results are shown (n = 3).

The pharmacokinetic parameters were calculated using a non-compartment model. The $AUC_{0-\infty}$ of paclitaxel after glucose-paclitaxel nanomicelle administration was over 3-fold higher than that of the paclitaxel solution, which could be beneficial for drug accumulation at the tumor site. Although the plasma content of paclitaxel was higher in the elimination phase after glucose-paclitaxel nanomicelle administration, the rate of clearance was only one-third of that of paclitaxel solution, potentially due to the resistance to drug clearance provided by nanomicelles. Additionally, the volume of distribution, V_z was 3.074 ± 0.314 L/kg, which is approximately half that of the paclitaxel solution.

In vivo Toxicity Assay

Blood cells were measured for leukocyte count (reference ranges 2.31~12.16 $\times 10^9$/L), lymphocyte count (reference ranges 1.90~11.04 $\times 10^9$/L), erythrocyte count (reference ranges 5.45~8.42 $\times 10^9$/L), hemoglobin concentration (reference

https://doi.org/10.2147/IJN.S500999

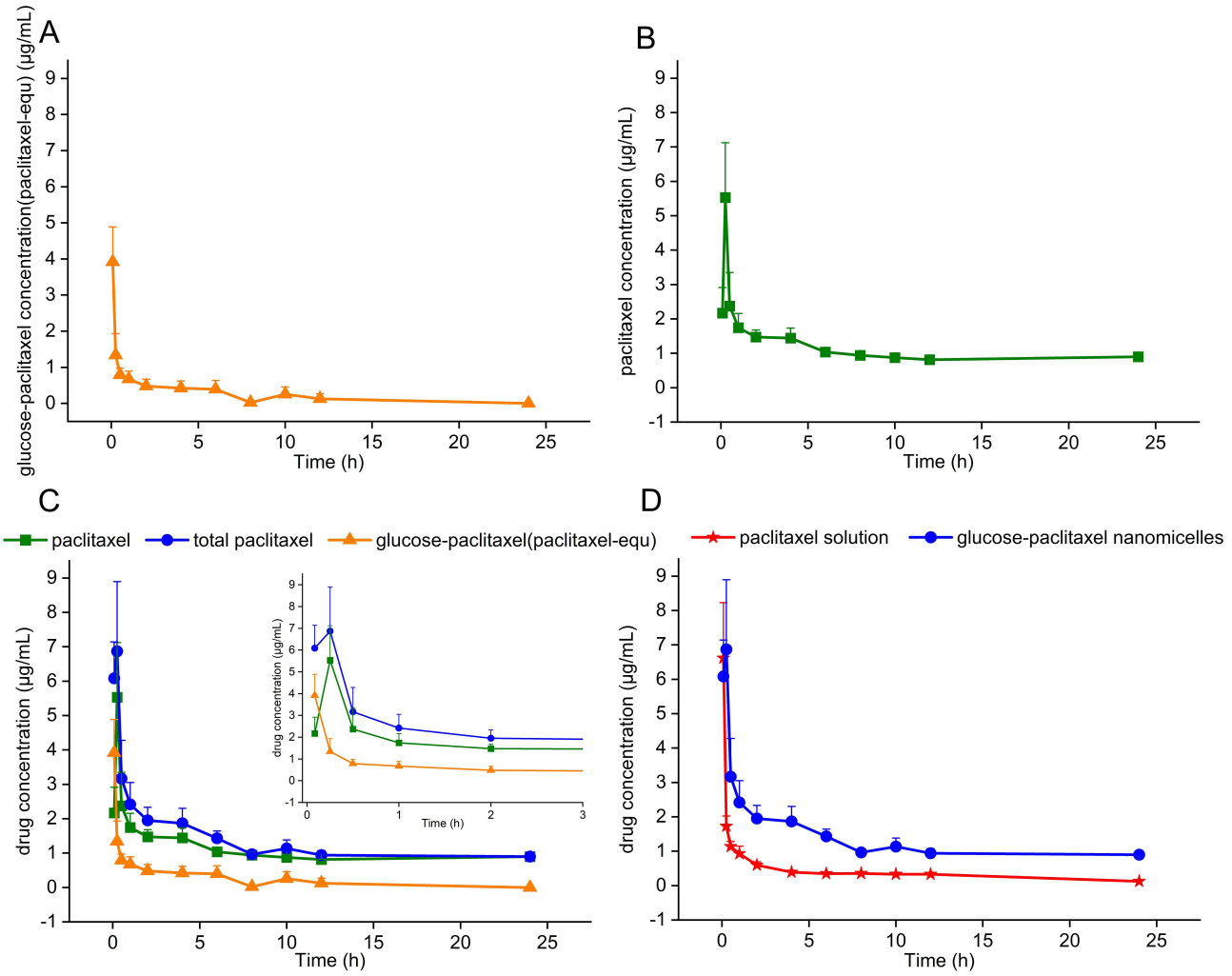

Figure 7 (**A**) Plasma concentration of glucose-paclitaxel over time after glucose-paclitaxel nanomicelles administration; (**B**) Plasma concentration of paclitaxel over time after glucose-paclitaxel nanomicelles administration; (**C**) Plasma concentration of paclitaxel, glucose-paclitaxel, total paclitaxel over time after glucose-paclitaxel nanomicelles administration; (**D**) Plasma concentration of paclitaxel over time after paclitaxel solution or glucose-paclitaxel nanomicelles administration. Data expression: mean ± standard deviation (n = 3).

ranges 118.47~156.78 g/L), and neutrophil count (reference ranges 0.00~1.20 $\times 10^9$/L). Figure 8 illustrates the changes over time following a single dose of either paclitaxel solution or glucose-paclitaxel nanomicelles. Among these types of blood cells, neutrophils increased after the administration of both formulations, showing significant differences at the 12-

Table 2 Pharmacokinetic Parameters After Paclitaxel Solution and Glucose-Paclitaxel Nanomicelles Administration to SD Rats (n = 3)

PK parameters	Paclitaxel solution	Glucose-paclitaxel nanomicelles	
	Paclitaxel	Glucose-paclitaxel	Total paclitaxel
$t_{1/2z}$ (h)	10.149 ± 0.310	4.290 ± 1.089**	22.781 ± 14.756
AUC_{0-t} (mg/L·h)	9.405 ± 0.397	6.544 ± 3.364	31.239 ± 4.695**
$AUC_{0-\infty}$ (mg/L·h)	11.201 ± 0.528	8.211 ± 4.828	58.712 ± 24.041*
V_z (L/kg)	6.541 ± 0.149	4.248 ± 1.287*	2.620 ± 0.755**
CL_z (L/h/kg)	0.447 ± 0.022	0.742 ± 0.347	0.098 ± 0.048**
$MRT_{0-\infty}$ (h)	12.223 ± 0.374	5.694 ± 1.931**	34.426 ± 17.375

Note: *p < 0.05, **p < 0.01.

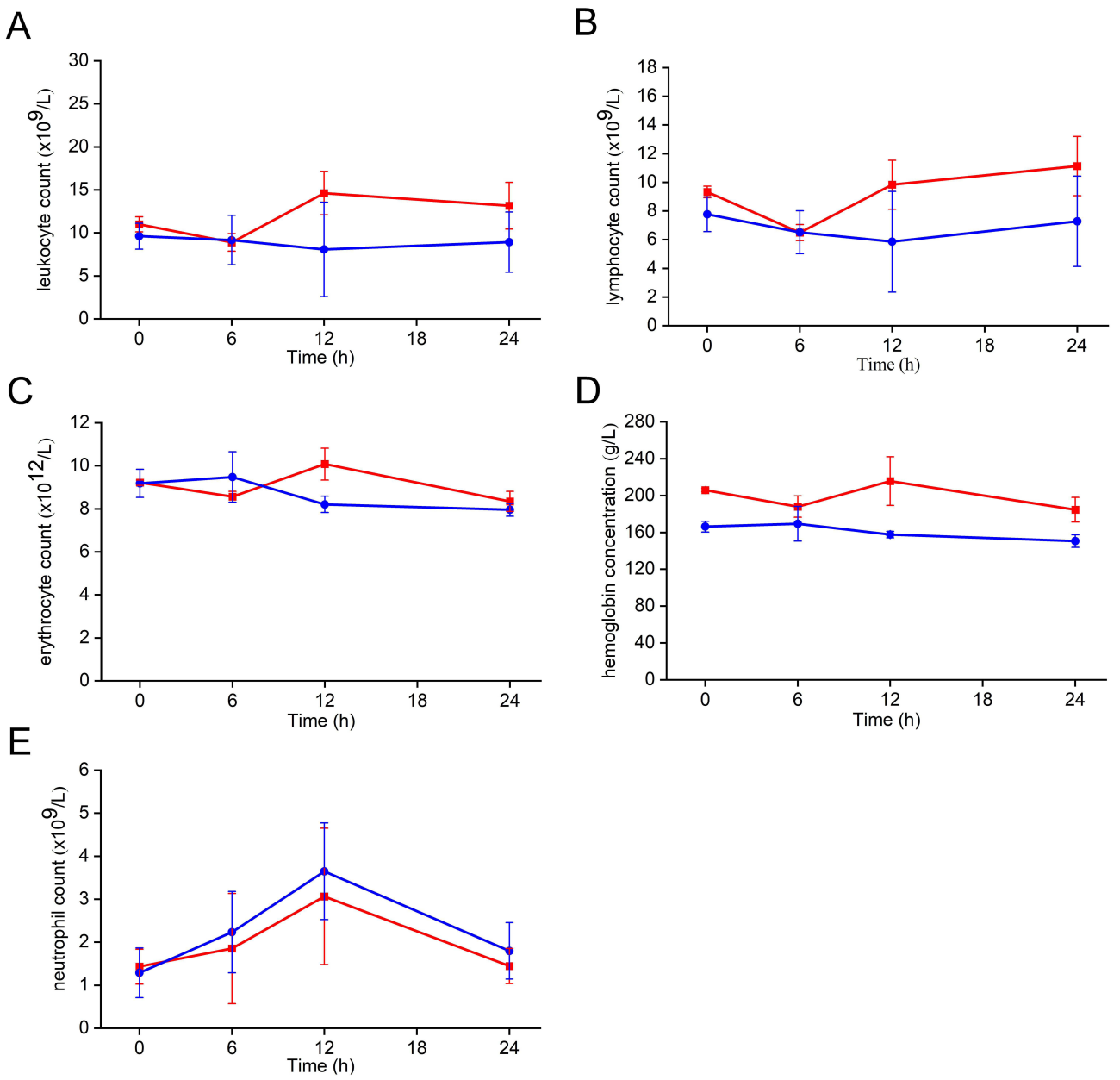

Figure 8 The changes of blood cells over time post-administrations of paclitaxel solution (●) or glucose-paclitaxel nanomicelles (■) (n=3). (**A**) leukocyte count; (**B**) lymphocyte count; (**C**) erythrocyte count; (**D**) hemoglobin concentration; (**E**) neutrophil count.

hour mark compared to the baseline ($p < 0.01$) (Figure 9). The neutrophil count remained higher after paclitaxel solution administration than after glucose-paclitaxel nanomicelle administration, despite the insignificant difference ($p > 0.05$).

The tail-flick latency after a single dose of paclitaxel solution or glucose-paclitaxel nanomicelles administration is depicted in Figure 10, which was significantly prolonged after paclitaxel solution administration ($p < 0.05$) and was notably longer than the latency observed following administration of glucose-paclitaxel nanomicelles.

Discussion

The effectiveness and safety of paclitaxel are two sides of the same coin, and losing balance on either side can cause the coin to fall and fail in clinical trials.[41,42] Taxol®, the first generic product of paclitaxel, has demonstrated antitumor activity in cervical, breast, ovarian, and lung cancers. It has also been associated with hypersensitivity reactions and nonlinear pharmacokinetics caused by co-solvent mixtures. Subsequent formulations of paclitaxel, such as Abraxane,[26]

https://doi.org/10.2147/IJN.S500999

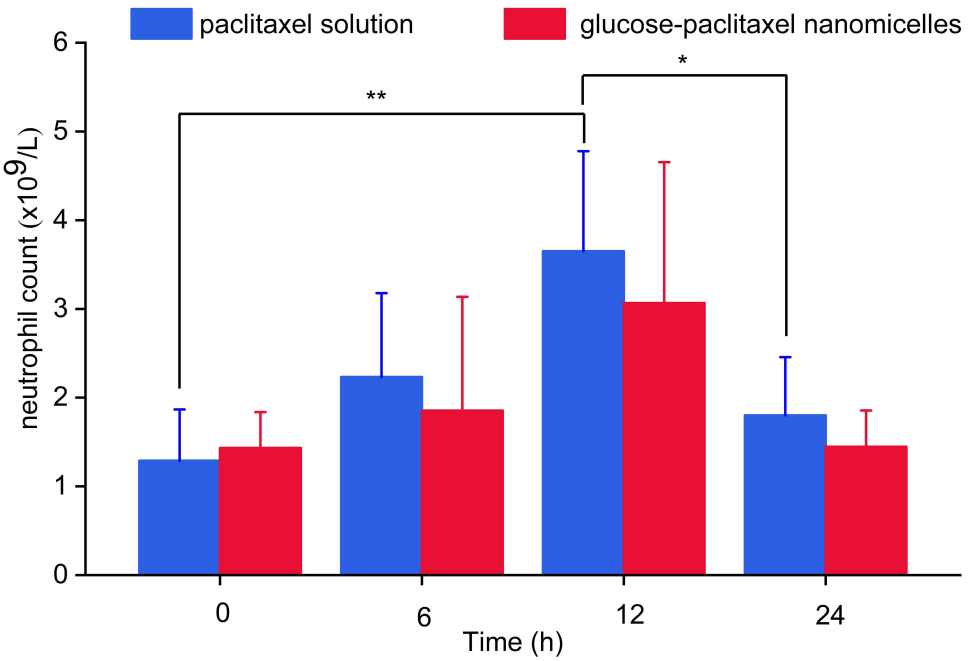

Figure 9 Neutrophil count after paclitaxel solution and glucose-paclitaxel nanomicelles administrations (*$p < 0.05$, **$p < 0.01$).

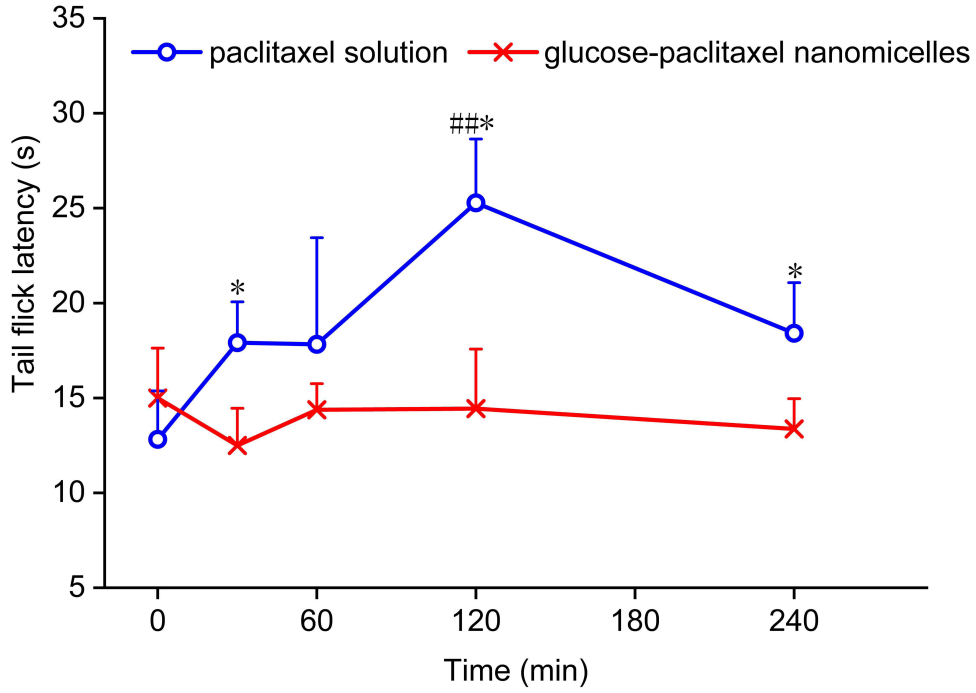

Figure 10 The tail-flick latency after administrations of paclitaxel solution and glucose-paclitaxel nanomicelles (*vs paclitaxel solution $p < 0.05$ and ##vs before paclitaxel solution treatment $p < 0.01$).

Genexol-PM,[11] and NK105,[10] have been reformed to remove CrEL, achieving benefits compared to Taxol® in clinical trials. However, several new paclitaxel formulations have failed in clinical trials because of the increased incidence of blood-system disorders and peripheral neuropathy.[19,22,43,44] Therefore, the design of paclitaxel formulations must consider the potential impacts of these two toxic side effects.

To reduce the toxic side effects of paclitaxel, a glucose-paclitaxel prodrug linked by succinic acid was synthesized and encapsulated in nanomicelles. This strategy enhanced drug solubility and eliminated the need for CrEL. Glucose-paclitaxel conjugates were converted to paclitaxel mainly in the blood, with a half-life time of 8.59 minutes, which could be delayed after encapsulation in nanomicelles. In SD rats, the in vivo plasma glucose-paclitaxel concentration rapidly decreased after drug administration, with levels approaching the quantitation limit at 12 hours. During this process, plasma glucose-paclitaxel may have three fates: 1) conversion to paclitaxel, 2) distribution to tissues, and 3) excretion from the body. Correspondingly, plasma paclitaxel concentration peaked at C_{max} within 15 min of the initial increase.

The pharmacokinetic behavior of glucose-paclitaxel nanomicelles was significantly altered in SD rats compared to that in paclitaxel solution. Starting 15 min post-administration, the plasma concentration of glucose-paclitaxel nanomicelles remained significantly higher than that of the paclitaxel solution, and V_z was only 40% of the paclitaxel solution. The reduced distribution of the drug to the tissues was conducive to peripheral neuropathy management,[20,22] consequently, the tail-flick latency in SD rats receiving glucose-paclitaxel nanomicelles was shorter than that in the paclitaxel solution group. In contrast, the encapsulation of glucose-paclitaxel by nanomicelles resulted in a 4-fold decrease in drug clearance and a 5-fold increase in AUC, however, this did not result in excessive exposure to high concentrations of free paclitaxel in the bloodstream. As shown by the results related to blood system disorders, the change in neutrophil count after glucose-paclitaxel nanomicelle administration was lower than that observed with the paclitaxel solution. This may be attributed to the prodrug and nanomicelles, which reduce the likelihood of free paclitaxel coming into direct contact with the bone marrow.[45]

In summary, the glucose-paclitaxel conjugate encapsulated in nanomicelles improved the water solubility of the parent drug, and significantly changed the pharmacokinetic behavior comparing with paclitaxel solution. These changes directly affected the toxicity of glucose-paclitaxel nanomicelles in rats, showing a reduction of paclitaxel toxicity to the hematological system and peripheral nervous system.

Conclusions

In this study, we propose that paclitaxel formulation design should focus on controlling blood-system disorders and peripheral neuropathy. To achieve this, a glucose-paclitaxel conjugate was synthesized and encapsulated in nanomicelles. Glucose-paclitaxel nanomicelles enhance the water solubility of paclitaxel and improve the stability of the glucose-paclitaxel conjugate. The pharmacokinetic behavior of glucose-paclitaxel nanomicelles was significantly altered in SD rats compared to that in paclitaxel solution. Finally, glucose-paclitaxel nanomicelles mitigate paclitaxel toxicity to the hematological system and peripheral nervous system in SD rats. This formulation strategy provides a solution to the failure of paclitaxel formulations owing to the dose-limiting toxicity induced by paclitaxel itself in clinical trials.

Data Sharing Statement

Original data remains available, raising proper quest to corresponding author for details.

Ethics Approval and Institutional Review Board Statement

All animal studies were conducted in accordance with the guidelines for the ethical review of laboratory animal welfare (Chinese National Standard GB/T 35892-2018),[46] and complied with the regulations and guidelines care set forth by Southwest Medical University. The studies were approved by the Experimental Animal Ethics Committee of the Southwest Medical University (20230216-003, approval date: February 16, 2023).

Funding

This work was funded by the Natural Science Foundation of Hebei Province and the Biological Medicine Joint Fund of the Natural Science Foundation of Hebei Province (H2019208339 and H2021208011), with a performance grant from the Hebei Research Center of Pharmaceutical and Chemical Engineering (225676121H).

Disclosure

No conflicts of interest were reported.

References

1. Liu J, Zhang Y, Liu C, Jiang Y, Wang Z, Li X. Paclitaxel prodrug-encapsulated polypeptide micelles with redox/pH dual responsiveness for cancer chemotherapy. *Int J Pharm*. 2023;645:123398. doi:10.1016/j.ijpharm.2023.123398
2. Stage TB, Bergmann TK, Kroetz DL. Clinical pharmacokinetics of paclitaxel monotherapy: an updated literature review. *Clin Pharmacokinet*. 2018;57(1):7–19. doi:10.1007/s40262-017-0563-z
3. Arbour KC, Mezquita L, Long N, et al. Impact of baseline steroids on efficacy of programmed cell death-1 and programmed death-ligand 1 blockade in patients with non-small-cell lung cancer. *J Clin Oncol*. 2018;36(28):2872–2878. doi:10.1200/jco.2018.79.0006
4. Waugh WN, Trissel LA, Stella VJ. Stability, compatibility, and plasticizer extraction of taxol (NSC-125973) injection diluted in infusion solutions and stored in various containers. *Am J Hosp Pharm*. 1991;48(7):1520–1524.
5. Sparreboom A, van Zuylen L, Brouwer E, et al. Cremophor EL-mediated alteration of paclitaxel distribution in human blood: clinical pharmacokinetic implications. *Cancer Res*. 1999;59(7):1454–1457.
6. Henningsson A, Karlsson MO, Viganò L, Gianni L, Verweij J, Sparreboom A. Mechanism-based pharmacokinetic model for paclitaxel. *J Clin Oncol*. 2001;19(20):4065–4073. doi:10.1200/jco.2001.19.20.4065
7. Williamson SK, Johnson GA, Maulhardt HA, et al. A phase I study of intraperitoneal nanoparticulate paclitaxel (Nanotax®) in patients with peritoneal malignancies. *Cancer Chemother Pharmacol*. 2015;75(5):1075–1087. doi:10.1007/s00280-015-2737-4
8. Thomas JS, Habib D, Hanna DL, et al. A Phase 1 trial of FID-007, a novel nanoparticle paclitaxel formulation, in patients with solid tumors. *J Clin Oncol*. 2021;39(15_suppl):3021. doi:10.1200/JCO.2021.39.15_suppl.3021
9. Armstrong DK, Fleming GF, Markman M, Bailey HH. A phase I trial of intraperitoneal sustained-release paclitaxel microspheres (Paclimer) in recurrent ovarian cancer: a Gynecologic Oncology Group study. *Gynecol Oncol*. 2006;103(2):391–396. doi:10.1016/j.ygyno.2006.02.029
10. Fujiwara Y, Mukai H, Saeki T, et al. A multi-national, randomised, open-label, parallel, Phase III non-inferiority study comparing NK105 and paclitaxel in metastatic or recurrent breast cancer patients. *Br J Cancer*. 2019;120(5):475–480. doi:10.1038/s41416-019-0391-z
11. Park IH, Sohn JH, Kim SB, et al. An open-label, randomized, parallel, phase III trial evaluating the efficacy and safety of polymeric micelle-formulated paclitaxel compared to conventional cremophor EL-based paclitaxel for recurrent or metastatic HER2-negative breast cancer. *Cancer Res Treat*. 2017;49(3):569–577. doi:10.4143/crt.2016.289
12. Vergote I, Bergfeldt K, Franquet A, et al. A randomized phase III trial in patients with recurrent platinum sensitive ovarian cancer comparing efficacy and safety of paclitaxel micellar and Cremophor EL-paclitaxel. *Gynecol Oncol*. 2020;156(2):293–300. doi:10.1016/j.ygyno.2019.11.034
13. Ranade AA, Bapsy PP, Nag S, et al. A multicenter Phase II randomized study of Cremophor-free polymeric nanoparticle formulation of paclitaxel in women with locally advanced and/or metastatic breast cancer after failure of anthracycline. *Asia Pac J Clin Oncol*. 2013;9(2):176–181. doi:10.1111/ajco.12035
14. Shi M, Gu A, Tu H, et al. Comparing nanoparticle polymeric micellar paclitaxel and solvent-based paclitaxel as first-line treatment of advanced non-small-cell lung cancer: an open-label, randomized, multicenter, phase III trial. *Ann Oncol*. 2021;32(1):85–96. doi:10.1016/j.annonc.2020.10.479
15. Slingerland M, Guchelaar HJ, Rosing H, et al. Bioequivalence of liposome-entrapped paclitaxel easy-to-use (LEP-ETU) formulation and paclitaxel in polyethoxylated castor oil: a randomized, two-period crossover study in patients with advanced cancer. *Clin Ther*. 2013;35(12):1946–1954. doi:10.1016/j.clinthera.2013.10.009
16. Strieth S, Dunau C, Michaelis U, et al. Phase I/II clinical study on safety and antivascular effects of paclitaxel encapsulated in cationic liposomes for targeted therapy in advanced head and neck cancer. *Head Neck*. 2014;36(7):976–984. doi:10.1002/hed.23397
17. Zhang J, Pan Y, Shi Q, et al. Paclitaxel liposome for injection (Lipusu) plus cisplatin versus gemcitabine plus cisplatin in the first-line treatment of locally advanced or metastatic lung squamous cell carcinoma: a multicenter, randomized, open-label, parallel controlled clinical study. *Cancer Commun*. 2022;42(1):3–16. doi:10.1002/cac2.12225
18. Choi M, Hsu J, Trieu V. Abstract CT315: IG-002 Phase 3 data: absence of correlation between unbound paclitaxel and response in MBC. *Cancer Res*. 2014;74(19 Supplement):CT315–CT315. doi:10.1158/1538-7445.AM2014-CT315
19. Bedikian AY, DeConti RC, Conry R, et al. Phase 3 study of docosahexaenoic acid-paclitaxel versus dacarbazine in patients with metastatic malignant melanoma. *Ann Oncol*. 2011;22(4):787–793. doi:10.1093/annonc/mdq438
20. Drappatz J, Brenner A, Wong ET, et al. Phase I study of GRN1005 in recurrent malignant glioma. *Clin Cancer Res*. 2013;19(6):1567–1576. doi:10.1158/1078-0432.Ccr-12-2481
21. O'Brien ME, Socinski MA, Popovich AY, et al. Randomized phase III trial comparing single-agent paclitaxel Poliglumex (CT-2103, PPX) with single-agent gemcitabine or vinorelbine for the treatment of PS 2 patients with chemotherapy-naïve advanced non-small cell lung cancer. *J Thorac Oncol*. 2008;3(7):728–734. doi:10.1097/JTO.0b013e31817c6b68
22. Kundranda MN, Niu J. Albumin-bound paclitaxel in solid tumors: clinical development and future directions. *Drug Des Devel Ther*. 2015;9:3767–3777. doi:10.2147/DDDT.S88023
23. Ibrahim NK, Desai N, Legha S, et al. Phase I and pharmacokinetic study of ABI-007, a Cremophor-free, protein-stabilized, nanoparticle formulation of paclitaxel. *Clin Cancer Res*. 2002;8(5):1038–1044.
24. Nyman DW, Campbell KJ, Hersh E, et al. Phase I and pharmacokinetics trial of ABI-007, a novel nanoparticle formulation of paclitaxel in patients with advanced nonhematologic malignancies. *J Clin Oncol*. 2005;23(31):7785–7793. doi:10.1200/jco.2004.00.6148
25. Sparreboom A, Scripture CD, Trieu V, et al. Comparative preclinical and clinical pharmacokinetics of a cremophor-free, nanoparticle albumin-bound paclitaxel (ABI-007) and paclitaxel formulated in Cremophor (Taxol). *Clin Cancer Res*. 2005;11(11):4136–4143. doi:10.1158/1078-0432.Ccr-04-2291
26. Gradishar WJ, Tjulandin S, Davidson N, et al. Phase III trial of nanoparticle albumin-bound paclitaxel compared with polyethylated castor oil-based paclitaxel in women with breast cancer. *J Clin Oncol*. 2005;23(31):7794–7803. doi:10.1200/jco.2005.04.937
27. Kurzrock R, Gabrail N, Chandhasin C, et al. Safety, pharmacokinetics, and activity of GRN1005, a novel conjugate of angiopep-2, a peptide facilitating brain penetration, and paclitaxel, in patients with advanced solid tumors. *mol Cancer Ther*. 2012;11(2):308–316. doi:10.1158/1535-7163.Mct-11-0566
28. Fetterly GJ, Grasela TH, Sherman JW, et al. Pharmacokinetic/pharmacodynamic modeling and simulation of neutropenia during phase I development of liposome-entrapped paclitaxel. *Clin Cancer Res*. 2008;14(18):5856–5863. doi:10.1158/1078-0432.Ccr-08-1046

29. Fetterly GJ, Tamburlin JM, Straubinger RM. Paclitaxel pharmacodynamics: application of a mechanism-based neutropenia model. *Biopharm Drug Dispos*. 2001;22(6):251–261. doi:10.1002/bdd.283
30. Friberg LE, Henningsson A, Maas H, Nguyen L, Karlsson MO. Model of chemotherapy-induced myelosuppression with parameter consistency across drugs. *J Clin Oncol*. 2002;20(24):4713–4721. doi:10.1200/jco.2002.02.140
31. Mielke S, Sparreboom A, Steinberg SM, et al. Association of Paclitaxel pharmacokinetics with the development of peripheral neuropathy in patients with advanced cancer. *Clin Cancer Res*. 2005;11(13):4843–4850. doi:10.1158/1078-0432.Ccr-05-0298
32. Scripture CD, Figg WD, Sparreboom A. Peripheral neuropathy induced by paclitaxel: recent insights and future perspectives. *Curr Neuropharmacol*. 2006;4(2):165–172. doi:10.2174/157015906776359568
33. Gonzalez P, Debnath S, Chen YA, et al. A theranostic small-molecule prodrug conjugate for neuroendocrine prostate cancer. *Pharmaceutics*. 2023;15(2):481. doi:10.3390/pharmaceutics15020481
34. Pastuch-Gawołek G, Szreder J, Domińska M, Pielok M, Cichy P, Grymel M. A small sugar molecule with huge potential in targeted cancer therapy. *Pharmaceutics*. 2023;15(3). doi:10.3390/pharmaceutics15030913
35. Mao Y, Zhang Y, Luo Z, et al. Synthesis, biological evaluation and low-toxic formulation development of glycosylated paclitaxel prodrugs. *Molecules*. 2018;23(12):3211. doi:10.3390/molecules23123211
36. Meng X, Lian X, Li X, et al. Synthesis of 2'-paclitaxel 2-deoxy-2-fluoro-glucopyranosyl carbonate for specific targeted delivery to cancer cells. *Carbohydr Res*. 2020;493:108034. doi:10.1016/j.carres.2020.108034
37. Sinani G, Durgun ME, Cevher E, Özsoy Y. Polymeric-micelle-based delivery systems for nucleic acids. *Pharmaceutics*. 2023;15(8):2021. doi:10.3390/pharmaceutics15082021
38. Radeva L, Yordanov Y, Spassova I, Kovacheva D, Tzankova V, Yoncheva K. Double-loaded doxorubicin/resveratrol polymeric micelles providing low toxicity on cardiac cells and enhanced cytotoxicity on lymphoma cells. *Pharmaceutics*. 2023;15(4):1287. doi:10.3390/pharmaceutics15041287
39. Landry KK, Lyon JL, Victoria KE, et al. Weekly vs every-3-week carboplatin with weekly paclitaxel in neoadjuvant chemotherapy for triple-negative breast cancer: a retrospective analysis. *Breast Cancer*. 2022;15(14). doi:10.2147/BCTT.S342635
40. Li Y, Wu Y, Fang Z, et al. Dendritic nanomedicine with boronate bonds for augmented chemo-immunotherapy via synergistic modulation of tumor immune microenvironment. *Adv Mater*. 2024;36(2). doi:10.1002/adma.202307263
41. Gallego-Jara J, Lozano-Terol G, Sola-Martínez RA, Cánovas-Díaz M, de Diego Puente T. A compressive review about taxol(®): history and future challenges. *Molecules*. 2020;25(24):5986. doi:10.3390/molecules25245986
42. Haddad R, Alrabadi N, Altaani B, Li T. Paclitaxel drug delivery systems: focus on nanocrystals' surface modifications. *Polymers (Basel)*. 2022;14(4):658. doi:10.3390/polym14040658
43. Meerum Terwogt JM, ten Bokkel Huinink WW, Schellens JH, et al. Phase I clinical and pharmacokinetic study of PNU166945, a novel water-soluble polymer-conjugated prodrug of paclitaxel. *Anticancer Drugs*. 2001;12(4):315–323. doi:10.1097/00001813-200104000-00003
44. Pavel M, Schuppan D, Jost L, et al. 1473 POSTER Tocosol® paclitaxel and cremophorel®-paclitaxel: the pharmacokinetic comparison shows that a new paclitaxel formulation leads to increased drug exposure. *EJC Suppl*. 2005;3(2):427. doi:10.1016/S1359-6349(05)81764-1
45. Liu J, Bai Y, Li Y, Li X, Luo K. Reprogramming the immunosuppressive tumor microenvironment through nanomedicine: an immunometabolism perspective. *EBioMedicine*. 2024;107:105301. doi:10.1016/j.ebiom.2024.105301
46. MacArthur Clark JA, Sun D. Guidelines for the ethical review of laboratory animal welfare People's Republic of China national standard GB/T 35892-2018 [Issued 6 February 2018 effective from 1 September 2018]. *Animal Model Exp Med*. 2020;3(1):103–113. doi:10.1002/ame2.12111